JOURNAL OF GEOPHYSICAL RESEARCH, VOL. 106, NO. C12, PAGES 31,303–31,318, DECEMBER 15, 2001

Computing optimum estuarine residual fluxes with a multiparameter inverse method (OERFIM): application to the Ria de Vigo (NW Spain)

M. Gilcoto[1], X.A. Álvarez–Salgado, F.F. Pérez

Instituto de Investigacións Mariñas, Consejo Superior de Investigaciones Científicas (CSIC), Vigo, Spain

Abstract. OERFIM is a two-dimensional (2-D) multiparameter inverse method for calculating estuarine residual fluxes and net ecosystem production rates in estuaries and coastal inlets. OERFIM retains the optimum solution for a weighted system of property conservation equations following the mean squares criterion. The properties involved are volume, salinity, temperature, nutrients (NH_4^+, NO_2^-, NO_3^{-2}, and PO_4^{-3}), dissolved oxygen, and inorganic carbon. Derived variables such as NO, CO, PO, NCO, and PCO are also considered. OERFIM lies between optimum multiparameter analysis and inverse general ocean circulation models. The simplicity of the method allows for derivation of analytical solutions and a clear exposition of the estuarine box models evolution: from the pioneer, just determined Knudsen method to the overdetermined models such as OERFIM. The theoretical analysis also provides a coherent presentation of analytical errors and their relation to the weights entering the equations. We validate the method with field data from the coastal upwelling system of the "Ría de Vigo", demonstrating that OERFIM results are suitable to understand the solution structure and, therefore, the whole system itself.

1. Introduction

Over the last 25 years, inverse methods have been a key tool for the understanding of (1) the steady state general ocean circulation [*Wunsch*, 1977, 1978; *Mercier*, 1986; *Grose et al.*, 1994], and (2) the complex mixing of water masses in the oceans [*Tomczak*, 1981; *Thompson and Edwards*, 1981; *Mackas et al.*, 1987]. Conservation of mass/volume, salinity, and temperature are combined with some dynamic equations (thermal wind relation, vorticity conservation, Bernoulli equation, etc.) to solve the ocean circulation inverse problem. The determination of the level of no motion is the main intricacy of the method [*Fiadeiro and Veronis*, 1982]. The conventional set of linear mixing equations involving the thermohaline properties, dissolved oxygen (O_2), and nutrient salts (NO_3^-,HPO_4^{2-}, and H_4SiO_4) are used in the case of the water mass mixing problem. Contrary to the thermohaline properties, dissolved oxygen and nutrient distributions are affected to some extent by organic matter mineralization processes [*Redfield et al.*, 1963]. The effect of mineralization can be overcome in the case of deep ocean waters mixing in a restricted area. However, when thermocline waters are considered or basin-scale mixing problems have to be solved, the nonconservative nature of the chemical tracers should be considered. A new term, accounting for the mineralization processes, has to be added to the set of linear equations [*Karstensen and Tomczak*, 1997], or the conservative chemical tracers "NO" (= $O_2 + R_N \times NO_3^-$) and "PO" (= $O_2 + R_P \times HPO_4^{2-}$) introduced by *Broecker* [1974] should replace O_2, NO_3^-, and HPO_4^{2-}. R_N and R_P are stoichiometric coefficients, constant with depth and basin [*Anderson and Sarmiento*, 1994]. Despite the previous classification, some authors have introduced chemical tracers to solve the ocean circulation problem [*Wunsch*, 1988; *Mazé et al.*, 1997], whereas others have proposed using dynamic equations (conservation of vorticity) for water mass mixing problems [*Tomczak*, 1999].

The circulation and mixing of water bodies in partially mixed estuaries and coastal inlets have been traditionally solved using estuarine box models [*Officer*, 1980]. They are just particular inverse problems. Classical estuarine box models are based on the equations of mass/volume and salinity conservation to describe the circulation of continental and ocean waters within the study system. We present here a simple inverse method (OERFIM), which also includes temperature and the chemical tracers, to obtain the two-dimensional residual horizontal water fluxes in partially mixed estuaries and coastal inlets. The resultant overdetermined system of linear equations is solved on the basis of the least squares criterion, the most extended in ocean circulation [*Wunsch*, 1996] and optimum multiparameter (OMP) analysis of water mass mixing inverse methods [*Tomczak*, 1999]. The relative simplicity of the problem (only two water bodies are mixing) allows us to partly avoid the complicated numerical machinery developed to solve inverse problems [*Wunsch, and Minster*, 1982; *Tarantola and Valette*, 1982] and shows the connection between classical estuarine box models and recent inverse methods. Therefore as in Wunsch's "eclectic ocean model", our system of equations merges the available physical and chemical information.

In this paper we describe the method (section 2), derive the diverse box model approaches to estuarine circulation in the literature as particular cases of our general formulation (section 3), study the robustness of the estimations (section 4), and apply the method to study the exchange fluxes in the "Ría de Vigo", a large coastal inlet in NW Spain (section 5).

[1]Also at Departament of Applied Physics, University of Vigo, Vigo, Spain.

Paper number 2000JC000665.
0148-0227/01/2000JC000665$09.00

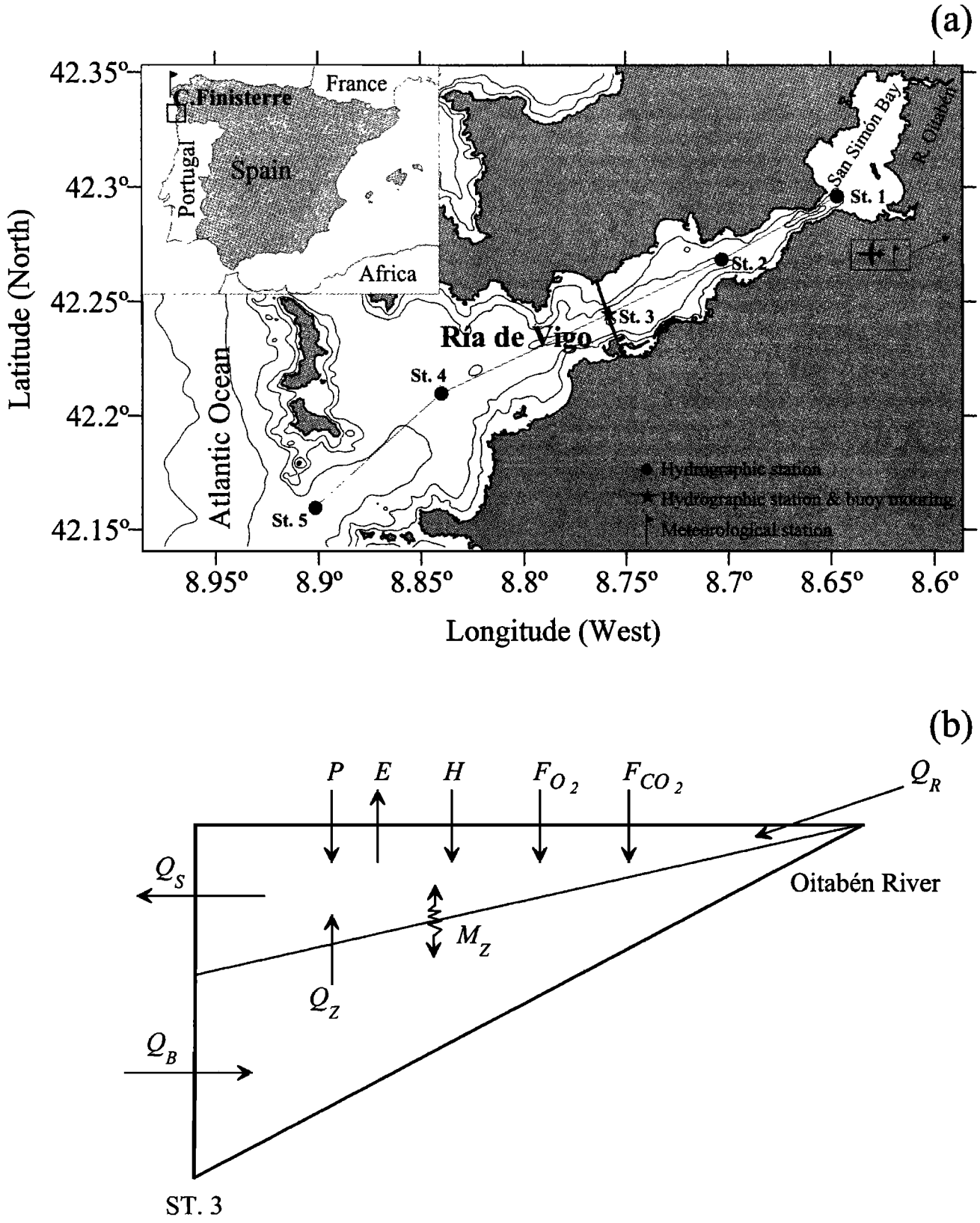

Figure 1. (a) Map of the "Ría de Vigo" (NW Spain), our study case, with the five sampling sites visited during September 1990 (solid circles) and the position of the remote monitoring buoy with suspended current meter and thermistor chain (solid star). The position of the meteorological observatories at Cape Finisterre and Vigo airport are also indicated. (b) Section across the main channel of the ría showing the study box with an open boundary at station 3. Abbreviations are as follows: Q_R, river discharge; E, evaporation rate; P, rainfall; H, atmospheric heat flux; F_{O_2}, atmospheric oxygen flux; F_{CO_2}, atmospheric carbon flux; and Q_B and Q_S, surface and bottom horizontal fluxes at the open boundary.

2. Inverse Method

The study partially mixed system is segmented in a certain number of enclosed volumes, known as "boxes", delimited by vertical sections perpendicular to the main axis of the system, known as "walls" (Figure 1a). The surrounding lands and the atmosphere also bound the boxes. A 2-D circulation pattern is assumed: The boxes are divided into two layers (surface and bottom), flowing in opposite directions (Figure 1b). The limit between the surface and bottom layer (level of no horizontal motion) is the gravity center of the boundary, that is, the depth where the actual density coincides with the average density of the boundary [*Rosón et al.*, 1997]. Equations of volume, heat (temperature), salinity, dissolved oxygen, inorganic carbon, and nutrient salt conservation are written for each box. Fluxes across all the boundaries, including continental inputs and air–sea exchange fluxes, are considered. In addition, net ecosystem production (NEP) rates, that is, the production of autotrophs minus the respiration of autotrophs and all heterotrophs within the box [*Smith and Hollibaugh*, 1997], are also included in the case of the nonconservative dissolved oxygen, inorganic carbon, and nutrient budgets. OERFIM computes optimum residual horizontal surface and bottom fluxes at the walls (Q_B and Q_S), as well as NEP rates within the boxes, between two consecutive surveys. Optimum vertical advection (Q_Z) and turbulent diffusion (M_Z) fluxes between the surface and bottom layer of each box can also be calculated. Application of OERFIM requires the direct measurement or the indirect estimation of the series of input variables listed below, which describe the thermohaline and chemical characteristics of each boundary and box.

2.1. Measured Variables

Full-depth profiles of salinity (S), temperature (T), dissolved oxygen (O_2), nitrate (NO_3^-), phosphate (HPO_4^{2-}), and two of the four carbon system variables (pH, total alkalinity (TA), total inorganic carbon (C_T), and CO_2 pressure (pCO_2)) are required. Ammonium (NH_4^+) and nitrite (NO_2^-) measurements are advisable in ecosystems where they contribute significantly to N nutrient variability. In addition, all these parameters have to be determined in the freshwater tributaries to the system. The temporal and spatial density of the sampling program will depend on the level of resolution required by the study problem. In parallel to the hydrographic program, key meteorological data such as local wind components (Wx, Wy), continental runoff (Q_R) precipitation rates (P), humidity (h), cloudiness (N), and air temperature (T_A) must be collected throughout the sampling period.

2.2. Variables Calculated From Collected Data

NEP rates of dissolved oxygen (ΔO_{2COR}) and inorganic carbon (ΔC_{TCOR}), nitrogen (ΔN_T) and phosphorus (ΔP_T) are linked by the Redfield's relationships:

$$\Delta O_{2COR} = -R_C \times \Delta C_{TCOR} = -R_N \times \Delta N_T = -R_P \times \Delta P_T, \quad (1)$$

R_C, R_N, and R_P are constant stoichiometric ratios of oxygen production (consumption) to inorganic carbon, nitrogen, and phosphorus consumption (production) during the synthesis (early degradation) of the organic tissues of marine phytoplankton. Consensus values for these molar ratios are R_C= 1.4, R_N= 9.5, and R_P= 150 for the average composition of phytoplankton organic matter: $C_{106}H_{175}O_{42}N_{16}P$, with 54.5% proteins, 25.5% carbohydrates, 16.1% lipids, and 4.0% nucleic acids [*Anderson*, 1995]. On the other hand, values of R_C= 1.4, R_N = 10.6, and R_P = 170 have been obtained by *Anderson and Sarmiento* [1994] from dissolved oxygen, inorganic carbon, and nutrient distributions in the world ocean at depths >400 m.

R_C, R_N and R_P are defined considering that NO_3^- is the inorganic nitrogen source (product) of phytoplankton photosynthesis (degradation). NH_4^+ and NO_2^- consumption (production) during the synthesis (oxidation) of phytoplankton organic matter produces (consumes) less oxygen than NO_3^-, affecting R_N. This effect can be quantified using the oxygen correction (O_{2COR}) introduced by *Ríos et al.* [1989]:

$$O_{2COR} = O_2 - \frac{1}{2} \times NO_2^- - 2 \times NH_4^+. \quad (2)$$

Since 0.5 mol of oxygen is necessary to oxidize 1 mol of nitrite to nitrate and 2 mol of oxygen are required to oxidize 1 mol of ammonium to nitrate, oxygen changes are normalized as if all N_T (= $NH_4^+ + NO_2^- + NO_3^-$) consumed (produced) was in NO_3^- form.

Inorganic carbon is consumed (produced) during the synthesis (degradation) of organic matter and calcareous ($CaCO_3$) structures. Since R_C refers only to the synthesis/oxidation of the organic tissues of marine phytoplankton, the influence of the precipitation/dissolution of $CaCO_3$ must be corrected from C_T variability (C_{TCOR}). Several authors introduced the correction 0.5 (TA + NO_3^-) in oceanic waters [*Broecker and Peng*, 1982; *Takahashi et al.*, 1985]. However, in coastal waters the influence of NO_2^- and NH_4^+ should also be considered. According to the acid dissociation constant of NO_2 (4.4×10^{-5} at salinity 35 practical salinity units (psu) and temperature 20°C [*Spencer*, 1975]) only ~45% of NO_2 is dissociated at pH= 4.4 (TA titration end point). Consequently, TA decreases (increases) by 0.45 mol per mol of NO_2 produced (consumed). On the other hand, TA increases (decreases) mole by mole with NH_4^+ formation (consumption) by organic matter degradation, leading to the following expression for C_{TCOR}:

$$C_{TCOR} = C_T - \frac{1}{2} \cdot \left(TA + NO_3^- + 0.45 \times NO_2^- - NH_4^+\right). \quad (3)$$

C_{TCOR} is independent of the N nutrient form and the precipitation/dissolution of $CaCO_3$. Therefore the calculated O_{2COR} and C_{TCOR} should be used instead of the directly measured O_2 and C_T.

Integration of the differential expressions in equation (1) leads to a corrected version of Broecker's original "NO" (NO_{COR}), "PO" (PO_{COR}), and "CO" (CO_{COR}) parameters:

$$NO_{COR} = O_{2COR} + R_N \times N_T, \quad (4)$$

$$PO_{COR} = O_{2COR} + R_P \times P_T, \quad (5)$$

$$CO_{COR} = O_{2COR} + R_C \times C_{TCOR}. \quad (6)$$

NO_{COR}, PO_{COR}, and CO_{COR} are conservative parameters, independent of the synthesis/degradation of organic matter and the precipitation/dissolution of $CaCO_3$ occurring within the boxes. The conservation of these parameters is compromised by the inalterability of R_C, R_N, and R_P, that is, the composition of the products of synthesis and early degradation of phytoplankton. NO_{COR}, PO_{COR}, and CO_{COR} are valid for most applications. In any case, deviations from the average composition used to be related to a transient excess production (consumption) of carbohydrates under N nutrient limitation conditions. *Fraga et al.* [1992, 1999] corrected the

effect of an excess production (consumption) of carbohydrates with the conservative NCO and PCO parameters, linear combinations of NO_{COR}, PO_{COR}, and CO_{COR}:

$$NCO = NO_{COR} \times \left(1 - \frac{1}{R_C}\right) + CO_{COR} \times \frac{1}{R_C}, \quad (7)$$

$$PCO = PO_{COR} \times \left(1 - \frac{1}{R_C}\right) + CO_{COR} \times \frac{1}{R_C}. \quad (8)$$

Exchange fluxes across the air–sea interface require the calculation of the evaporation term (E,), which enters the volume budget, the net heat entry from the atmosphere (H), which enters the temperature budget, and the net O_2, CO_2, and nutrient entry from the atmosphere, which enter the corresponding tracer budgets. Parametric equations for $E=f(h, W, T_A, T_S, S_S)$ and $H=f(h, W, T_A, T_S, N)$ are available in the literature [e.g., *Alvarez–Salgado et al.*, 2001]. Although the atmospheric nutrient input can be neglected in most applications, O_2 and CO_2 fluxes (FO_2 and FCO_2) should be calculated with the following equations (in mol s^{-1}):

$$F_{O_2} = k_{O_2} \times (O_{2SAT} - O_{2S}) \times A, \quad (9)$$

$$F_{CO_2} = k_{CO_2} \times S_{CO_2} \times (pCO_{2ATM} - pCO_{2S}) \times A, \quad (10)$$

where k_{CO_2} and k_{O_2} are the CO_2 and O_2 piston velocities (m s^{-1}), calculated from local winds (W_X, W_Y) following *Woolf and Thorpe's* [1991] and *Kester's* [1975] equations, respectively. S_{CO_2} is the solubility of CO_2 in seawater (mmol m^{-3} μatm^{-1}), calculated from salinity and temperature with the equation of *Weiss* [1974]. O_{2SAT} is the oxygen concentration at saturation in surface waters (mmol m^{-3}), calculated from salinity and temperature with the equation of *UNESCO* [1985]. The parameter pCO_{2ATM} is the CO_2 pressure in the atmosphere (μatm). O_{2S} and pCO_{2S} are oxygen (mmol m^{-3}) and pCO_2 (μatm) levels in surface waters. A is the surface area of the box (m^2). For the case of the conservative chemical parameters, the net entry of NO_{COR} (F_{NO}) and PO_{COR} (F_{PO}) equals the net entry of O_2 (F_{O_2}) if nutrient inputs are neglected. The net entry of CO_{COR} is $F_{CO} = F_{O_2} + R_C \times F_{CO_2}$.

Finally, $F_{NCO} = F_{PCO} = F_{O_2} + F_{CO_2}$.

2.3. Overdetermined System of Linear Equations

In order to simplify the presentation of the system of linear equations, they will be written for a box with a unique open boundary (Figure 1b). This box extends from the inner reaches of the estuary to the wall where the horizontal exchange fluxes have to be calculated. A NEP rate is simultaneously obtained for the box. Subsequently, an equivalent system of linear equations can be written for the bottom layer of the box in order to obtain the vertical fluxes and the bottom NEP. Then, the surface NEP can be calculated by subtracting the bottom NEP from the box NEP. Finally, several boxes can be defined, depending on the location of the wall along the estuary, and the vertical fluxes and NEP for the volume enclosed between two walls can be obtained by the difference of the corresponding vertical and NEP rates. Therefore although the circulation of partially mixed estuaries and coastal inlets is a 2-D problem, it can be solved step by step, starting from a 0-D system with a unique open boundary, moving to a 1-D system with two layers, and then, considering a 2-D system with several boxes. We present here the detailed solution for the first step, the 0-D system.

The equations of volume, heat (temperature), salt, O_{2COR}, C_{TCOR}, N_T, and P_T conservation for any box with an unique open boundary are as follows:

$$\overline{Q_S} - \overline{Q_B} - \overline{Q_R} - \overline{P} + \overline{E} = r_Q, \quad (11)$$

$$\overline{Q_S} \times \overline{T_S} - \overline{Q_B} \times \overline{T_B} - \overline{Q_R} \times \overline{T_R} - \overline{H} - \overline{P} \times \overline{T_A} + V \times \frac{\Delta T}{\Delta t} = r_T, \quad (12)$$

$$\overline{Q_S} \times \overline{S_S} - \overline{Q_B} \times \overline{T_B} + V \times \frac{\Delta S}{\Delta t} = r_S, \quad (13)$$

$$\overline{Q_S} \times \overline{O_{2S}} - \overline{Q_B} \times \overline{O_{2B}} - \overline{Q_R} \times \overline{O_{2R}} - \overline{F_{O_2}} - \overline{P} \times \overline{O_{2A}} - \overline{NEP} + V \times \frac{\Delta O_2}{\Delta t} = r_{O_2}, \quad (14)$$

$$\overline{Q_S} \times \overline{C_{TS}} - \overline{Q_B} \times \overline{C_{TB}} - \overline{Q_R} \times \overline{C_{TR}} - \overline{P} \times \overline{C_{TA}} - \overline{F_{CO_2}} + \frac{1}{R_C} \times \overline{NEP} + V \times \frac{\Delta C_T}{\Delta t} = r_{C_T}, \quad (15)$$

$$\overline{Q_S} \times \overline{N_{TS}} - \overline{Q_B} \times \overline{N_{TB}} - \overline{Q_R} \times \overline{N_{TR}} - \overline{P} \times \overline{N_{TA}} + \frac{1}{R_N} \times \overline{NEP} + V \times \frac{\Delta N_T}{\Delta t} = r_{N_T}, \quad (16)$$

$$\overline{Q_S} \times \overline{P_{TS}} - \overline{Q_B} \times \overline{P_{TB}} - \overline{Q_R} \times \overline{P_{TR}} - \overline{P} \times \overline{P_{TA}} + \frac{1}{R_P} \times \overline{NEP} + V \times \frac{\Delta P_T}{\Delta t} = r_{P_T}, \quad (17)$$

where Q_S and Q_B (m^3 s^{-1}) are the average residual surface and bottom horizontal fluxes across the open boundary of the box between two consecutive surveys. Q_R, P, and E (m^3 s^{-1}) are the average continental runoff, precipitation and evaporation in the box between two consecutive surveys. T_S, T_B, T_R, and T_A (°C) are the average temperature of the surface and bottom flows across the open boundary of the box, the river flow, and the atmosphere between two consecutive surveys. ΔT Δt (°C s^{-1}) is the net rate of change in the heat content (temperature) of the box between two consecutive surveys. For the case of the S, O_{2COR}, C_{TCOR}, N_T, and P_T conservation equations, the meaning of the corresponding variables is the same as for temperature. V is the volume of the box. H (m^3 °C s^{-1}), F_{O_2} (mol O_2 s^{-1}), and F_{CO_2} (mol C s^{-1}) are the average heat, O_2, and CO_2 exchange fluxes across the air–sea interface between two consecutive surveys. Finally, NEP (mol O_2 s^{-1}) is the average net ecosystem production within the box between two consecutive surveys. Obviously, this term only appears in the equations of the nonconservative chemical parameters.

Some reasonable assumptions are implicit in this system of equations: (1) The volume of the box is constant because a mean tidal volume is considered. (2) The average heat flux across the surface layer of the open boundary, $\overline{Q_S \times T_S}$, is simplified as the product of $\overline{Q_S} \times \overline{T_S}$. The same is applicable to the bottom layer, and the river and precipitation fluxes. It is also valid for salinity, O_{2COR}, C_{TCOR}, N_T, and P_T. The simplification is based on the extreme variability of waters fluxes compared with property changes in most estuarine and coastal systems. (3) The salinity of continental water and

rainwater is set to zero. (4) Finally, the produced/consumed organic matter has the average composition of the organic tissues of marine phytoplankton.

The average temperature, salinity, O_{2COR}, C_{TCOR}, N_T, and P_T of the surface and bottom layer of the wall and the box are obtained by numeric integration of measured profiles, considering the geometric characteristics of the estuary. $\overline{Q_R}$, $\overline{P}$, $\overline{T_A}$, $\overline{T_R}$, and the chemical composition of the river flow are known from direct measurements (section 2.1). $\overline{H}$, $\overline{F_{O_2}}$, and $\overline{F_{CO_2}}$ are also estimated from measured variables (section 2.2). Therefore the system of seven linear equations has only three unknowns: $\overline{Q_S}$, $\overline{Q_B}$, and $\overline{\text{NEP}}$. Hereinafter, the overbar used to indicate average values of any variable between two consecutive surveys will be removed.

Since the system is overdetermined, the solution (Q_S, Q_B, and NEP) that minimizes the weighted sum of squared residuals of the seven equations ($\sum_{i=1}^{7} r_i^2 \times w_i^2$) can be retained. The r_i are the residuals of the volume (r_Q, $m^3\ s^{-1}$), heat (r_T, °C s^{-1}), salt (r_S, kg s^{-1}) O_{2COR}, (r_{O_2}), C_{TCOR} (r_{C_T}), N_T (r_{N_T}), and P_T (r_{P_T}, mol s^{-1}) budgets, partly caused by the simplifications above. The w_i are factors that (1) weight the conservation equations on the basis of the relative analytical accuracy of every measured parameter and (2) normalize the residuals to a common dimension ($m^3\ s^{-1}$). The corresponding factor for the heat budget is

$$w_T = \frac{|T_B - T_S|}{\varepsilon_T} \times \left(\sum_{j=1}^{n} (T_B - T_S)_j^2 \, / n \right)^{-1/2} = \frac{T_B - T_S}{\varepsilon_T} \times \xi_T^{-1}. \quad (18)$$

The weighting term $|T_B - T_S| / \varepsilon_T$ indicates the number of times that the temperature gradient at the wall exceeds the accuracy of the determination of temperature. The normalizing term $\xi_T = (\sum_{j=1}^{n} (T_B - T_S)_j^2 / n)^{1/2}$ is the square root of the squared temperature gradient at the study wall averaged over the whole set of time intervals considered (n). Equivalent normalizing–weighting terms can be written for S, O_{2COR}, C_{TCOR}, N_T, and P_T. Finally, a large value of the factor for the volume budget ($w_Q >$ tidal prism volume) is preferred to satisfy the desirable condition that the volume is accurately conserved ($r_Q = 0$).

O_{2COR}, C_{TCOR}, N_T, and P_T can be substituted by the conservative chemical parameters CO_{COR}, NO_{COR}, and PO_{COR}. Equations (14) to (17) should be replaced by

$$Q_S \times \text{CO}_S - Q_B \times \text{CO}_B - Q_R \times \text{CO}_{2R} - P \times \text{CO}_{2A} - (F_{O_2} + R_C \times F_{CO_2}) + V \times \frac{\Delta \text{CO}}{\Delta t} = r_{\text{CO}}, \quad (19)$$

$$Q_S \times \text{NO}_S - Q_B \times \text{NO}_B - Q_R \times \text{NO}_R - P \times \text{NO}_A - F_{O_2} + V \times \frac{\Delta \text{NO}}{\Delta t} = r_{\text{NO}}, \quad (20)$$

$$Q_S \times \text{PO}_S - Q_B \times \text{PO}_B - Q_R \times \text{PO}_R - P \times \text{PO}_A - F_{O_2} + V \times \frac{\Delta \text{PO}}{\Delta t} = r_{\text{PO}}. \quad (21)$$

In this case, an overdetermined system of six linear equations (volume, heat, salt, CO_{COR}, NO_{COR}, and PO_{COR}) and just two unknowns (Q_S and Q_B) has to be solved. The corresponding factors w_{CO}, w_{NO}, and w_{PO} are calculated as for the nonconservative chemical parameters.

Finally, for a system where an excess production/consumption of carbohydrates is significant, NCO and PCO can replace CO_{COR}, NO_{COR}, and PO_{COR}:

$$Q_S \times \text{NCO}_S - Q_B \times \text{NCO}_B - Q_R \times \text{NCO}_R - P \times \text{NCO}_A - (F_{O_2} + F_{CO_2}) + V \times \frac{\Delta \text{NCO}}{\Delta t} = r_{\text{NCO}}, \quad (22)$$

$$Q_S \times \text{PCO}_S - Q_B \times \text{PCO}_B - Q_R \times \text{PCO}_R - P \times \text{PCO}_A - (F_{O_2} + F_{CO_2}) + V \times \frac{\Delta \text{PCO}}{\Delta t} = r_{\text{PCO}}, \quad (23)$$

leading to an overdetermined system of five linear equations (volume, heat, salt, NCO, and PCO) and two unknowns (Q_S and Q_B).

As indicated at the beginning of this section, once optimum Q_S, Q_B, and NEP have been calculated from the overdetermined system of equations (11)–(17), an equivalent system of seven mass balance equations should be written for the bottom layer of the box in Figure 1b to obtain optimum Q_Z, M_Z, and bottom NEP. Surface NEP would then be calculated from the difference between the calculated NEP for the box and the NEP for the bottom layer. The same reasoning is applicable to the case of Q_Z and M_Z when the conservative chemical tracers are used.

3. OERFIM, a General Formulation of Box Models

Knudsen's hydrographic theorem (introduced by that author to estimate exchange fluxes between the Baltic and North Seas from salinity distributions in 1900 [*Neumann et al.*, 1967]) is the essence of box models. *Pritchard*'s [1969] formulation of salinity–based 2-D box models contributed to the wide use of this tool in partially mixed estuaries, coastal inlets, and enclosed seas [e.g., *Taft et al.*, 1978; *Officer*, 1980; *Matsukawa and Suzuki*, 1985; *Prego and Fraga*, 1992]. However, the robustness of salinity–based calculations in partially mixed systems is limited by the vertical salinity gradient, $S_B - S_S$. In many coastal systems (mainly during the summer period, when continental runoff decreases to extreme minimum values) the vertical salinity gradient is too brief to produce reliable fluxes. *Smith and Hollibaugh* [1997] found empirically that salinity differences <0.3 psu in Tomales Bay (California) resulted in anomalously large fluxes that they rejected. In these cases, it is mandatory to base box model calculations in the distribution of another conservative variable with sufficient vertical gradient. This is usually the case for temperature during the summer when strong vertical gradients, $T_B - T_S$, are created by heat transference from the atmosphere to the surface layer. *Minas et al.* [1986] combined temperature profiles and heat exchange fluxes to roughly estimate flushing times in the upwelling systems of NW Africa, California, and Peru. A further step was made by *Rosón et al.* [1997], who used parallel salinity and temperature profiles to calculate exchange fluxes in the Spanish rías. In this section we will derive these classical box model inverse methods as particular cases of OERFIM.

3.1. Knudsen's Hydrographic Theorem

A modified non steady state Knudsen's hydrographic theorem is the simplest formulation of our inverse method to

obtain water fluxes from salinity distributions, assuming volume and salt conservation. The unique solution for this system of two equations (equations (11) and (13)) with two unknowns, $(Q_S)_S$ and $(Q_B)_S$, is

$$(Q_S)_S = \frac{(Q_R + P - E) \times S_B + V \times \frac{\Delta S}{\Delta t}}{S_B - S_S}, \quad (24)$$

$$(Q_B)_S = (Q_S)_S - (Q_R + P - E). \quad (25)$$

Equivalent systems of two equations with two unknowns can be solved to obtain water fluxes from temperature distributions, assuming volume and heat conservation (equations (11) and (12)):

$$(Q_S)_T = \left[(Q_R + P - E) \times T_B - Q_R \times T_R - P \times T_A - H + V \times \frac{\Delta T}{\Delta t}\right] \times (T_B - T_S)^{-1}, \quad (26)$$

$$(Q_B)_T = (Q_S)_T - (Q_R + P - E), \quad (27)$$

and from the different conservative chemical variables: CO_{COR} (equations (11) and (19)), NO_{COR} (equations (11) and (20)) and PO_{COR} (equations (11) and (21)) or NCO (equations (11) and (22)) and PCO (equations (11) and (23)). For the exemplar case of PCO the solution is

$$(Q_S)_{PCO} = \left[(Q_R + P - E) \times PCO_B - Q_R \times PCO_R - P \times PCO_A - (F_{O_2} + F_{CO_2}) + V \times \frac{\Delta PCO}{\Delta t}\right] \times (PCO_B - PCO_S)^{-1}, \quad (28)$$

$$(Q_B)_{PCO} = (Q_S)_{PCO} - (Q_R + P - E). \quad (29)$$

3.2. Mass–Heat Weighted Inverse Method of Rosón *et al.* [1997]

Rosón et al. [1997] presented for the first time a mass–heat weighted 2-D box model. They used parallel salinity and temperature distributions under the assumptions of volume, heat, and salt conservation. They obtained the solution for this system of three equations ((11), (12) and (13)) with two unknowns that minimizes the sum of weighted square residuals. In addition, they also considered that volume is accurately conserved ($r_Q = 0$). Under these conditions

$$r_S \times \frac{S_B - S_S}{T_B - T_S} \times \left(\frac{w_S}{w_T}\right)^2 + r_T = 0, \quad (30)$$

and the analytical expressions for the optimum values of $(Q_S)_{S,T}$ and $(Q_B)_{S\,T}$ are

$$(Q_S)_{S,T} = (Q_S)_S \times f + (Q_S)_T \times (1 - f), \quad (31)$$

$$(Q_B)_{S\,T} = (Q_S)_{S,T} - (Q_R + P - E), \quad (32)$$

with

$$f = \frac{(S_B - S_S)^2}{(S_B - S_S)^2 + (T_B - T_S)^2 \times \left(\frac{w_T}{w_S}\right)^2}. \quad (33)$$

Rosón et al. [1997] defined w_S and w_T just as normalizing factors:

$$w_S = \left(\sum_{j=1}^{n} (S_B - S_S)_j^2 \Big/ n\right)^{-1/2} = \xi_S^{-1}, \quad (34)$$

$$w_T = \left(\sum_{j=1}^{n} (T_B - T_S)_j^2 \Big/ n\right)^{-1/2} = \xi_T^{-1}. \quad (35)$$

Therefore the final expression of f for this case is

$$f = \frac{(S_B - S_S)^2}{(S_B - S_S)^2 + (T_B - T_S)^2 \cdot \frac{\sum_{j=1}^{n} (S_B - S_S)_j^2}{\sum_{j=1}^{n} (T_B - T_S)_j^2}}, \quad (36)$$

The factor f, which varies between 0.0 and 1.0, indicates the relative contribution of the salt, $(Q_S)_S$, and temperature, $(Q_S)_T$, solutions to the optimum salt–heat weighted solution, $(Q_S)_{S,T}$. Figure 2a shows the 1987–1996 time series of $|S_B - S_S|$ and $|T_B - T_S|$ in the central segment of the "Ría de Vigo" (NW Spain), station 3 in our study case (Figure 1a). The corresponding time series of f (Figure 2b) was calculated with (36). Values of f close to 1.0 are obtained during the winter months, when the salinity gradient is quite pronounced and the temperature gradient homogenizes. On the contrary, values of f close to 0.0 are obtained during the summer period, when continental runoff is limited and the temperature gradient maximizes. Steep transitions from extreme values of f are observed during spring and autumn.

Using appropriate w_T (equation (18)) and w_S normalizing–weighting factors, f would have the following expression:

$$f = \frac{(S_B - S_S)^4}{(S_B - S_S)^4 + (T_B - T_S)^4 \cdot \frac{\sum_j (S_B - S_S)_j^2}{\sum_j (T_B - T_S)_j^2} \cdot \left(\frac{\varepsilon_S}{\varepsilon_T}\right)^2}, \quad (37)$$

which produces more abrupt transitions between extreme values of f (Figure 2c), because the influence of vertical gradients in the calculation of f is now elevated to the fourth power. The values of f calculated with equations (36) and (37) are compared in Figure 2d.

3.3. OERFIM Solutions for the Thermohaline and Conservative Chemical Variables

Optimum horizontal residual fluxes, obtained from temperature, salinity, CO_{COR}, NO_{COR}, and PO_{COR} distributions (equations (11), (12), (13), (19), (20) and (21)), using the appropriate normalizing–weighting factors and assuming that the volume is accurately conserved, display the following analytical expressions:

$$Q_S = \sum_{i=1}^{5} (Q_S)_i \times f_i, \quad (38)$$

$$Q_B = Q_S - (Q_R + P - E), \quad (39)$$

with

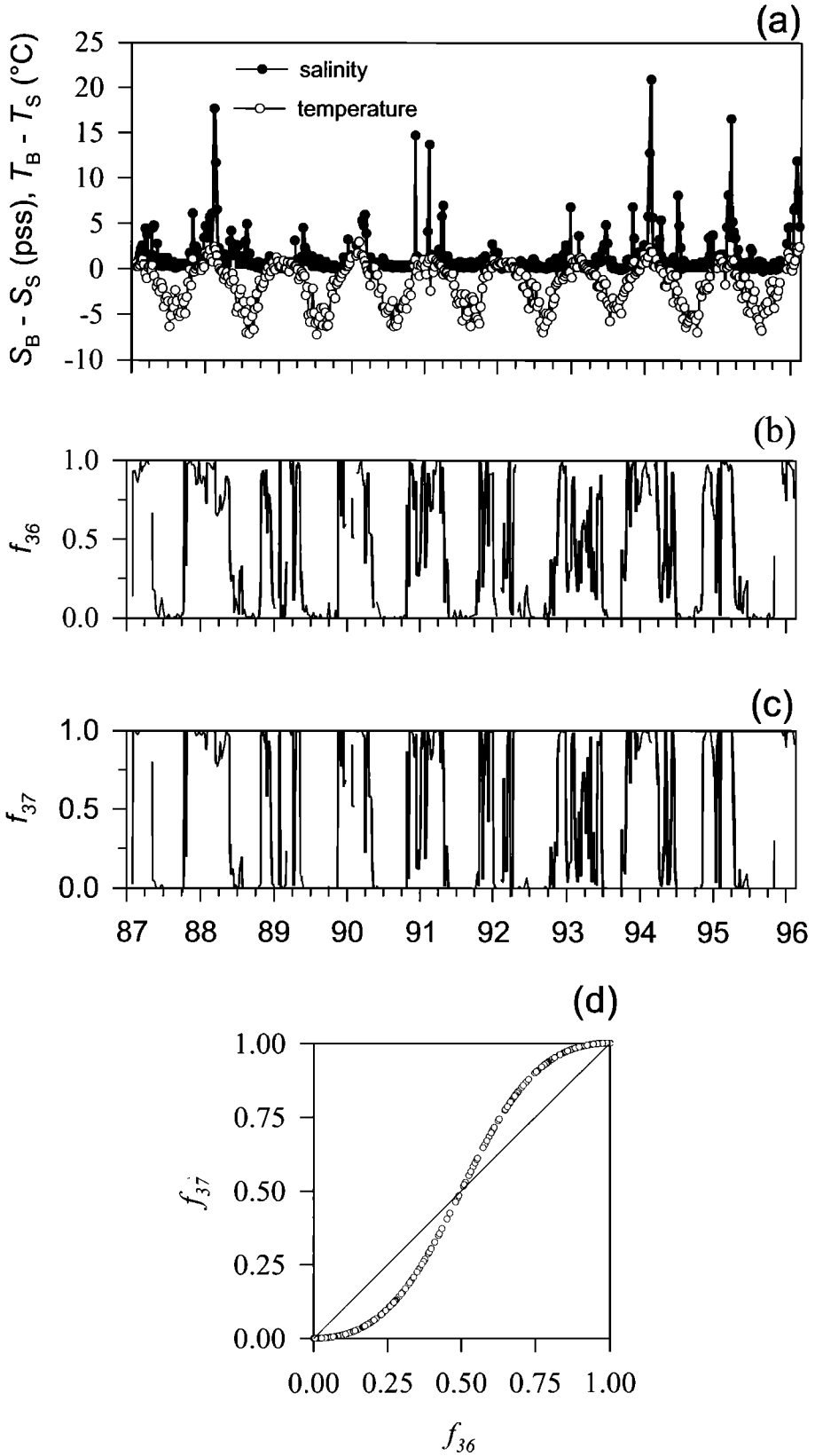

Figure 2. Time series of (a) $S_B - S_S$ and $T_B - T_S$, (b) the factor f calculated with equation (36), f_{36}, (c) the factor f calculated with equation (37), f_{37}, and (d) f_{36} versus f_{37} for station 3 ("Ría de Vigo", Figure 1), visited twice a week between 1987 and 1996.

$$f_i = \frac{(i_B - i_S)^2 \times w_i^2}{\sum_{i=1}^{5}(i_B - i_S)^2 \times w_i^2} \quad i = T, S, CO_{COR}, NO_{COR}, PO_{COR}. \quad (40)$$

Equivalent analytical expressions are obtained for the case of volume, salinity, temperature, NCO, and PCO conservation (equations (11), (12), (13), (22), (23)).

3.4. OERFIM Solutions for the Thermohaline and Nonconservative Chemical Variables

Consideration of the nonconservative chemical variables does not allow for easy derivation of simple analytical expressions for the optimum estuarine residual fluxes (Q_S and Q_B) and the net ecosystem production rates (NEP). The optimum solution for the system of equations (11)–(17) can be expressed in matrix form as follows:

$$\mathbf{Q} = (\mathbf{A}^T \times \mathbf{W}^2 \times \mathbf{A})^{-1} \times (\mathbf{A}^T \times \mathbf{W}^2 \times \mathbf{B}), \quad (41)$$

where $\boldsymbol{Q}$ is a 3×1 matrix containing the optimum multiparametric solution of this system of seven equations and three unknowns. $\boldsymbol{A}$ is a 7×3 matrix containing the chemical properties of Q_S and Q_B and the stoichiometric ratios of NEP. It is (1, –1, 0) for volume, (T_S, $-T_B$, 0) for temperature, (S_S, $-S_B$, 0) for salinity, (O_{2S}, $-O_{2B}$, –1) for O_{2COR}, (C_{TS}, $-C_{TB}$, $1/R_C$) for C_{TCOR}, (N_{TS}, $-N_{TB}$, $1/R_N$) for N_T and (P_{TS}, $-P_{TB}$, $1/R_P$) for P_T conservation. $\boldsymbol{W}$ is a 7×7 diagonal matrix containing w_Q, w_S, w_T, w_{O_2}, w_{C_T}, w_{N_T}, and w_{P_T}. And $\boldsymbol{B}$ is a 7×1 matrix containing the known river, air–sea exchange and accumulation terms. It is Q_R+P–E for volume, $Q_R \times T_R + P \times T_A + H - V \times \Delta T/\Delta t$ for temperature, $-V \times \Delta S/\Delta t$ for salinity, $Q_R \times O_{2R} + P \times O_{2A} + F_{O_2} - V \times \Delta O_2/\Delta t$ for O_{2COR}, $Q_R \times C_{TR} + P \times C_{TA} + F_{CO_2} - V \times \Delta C_T/\Delta t$ for C_{TCOR}, $Q_R \times N_{TR} + P \times N_{TA} - V \times \Delta N_T/\Delta t$ for N_T and $Q_R \times P_{TR} + P \times P_{TA} - V \times \Delta P_T/\Delta t$ for P_T conservation.

4. Robustness of the Estimated Fluxes

Horizontal residual flux calculations with 2-D inverse methods are constrained by the list of basic assumptions necessary to produce the inversion (e.g., 2-D approach, volume and properties conservation, etc.), which will affect the accuracy of the retained solution. This inaccuracy can only be assessed through validation with other "external" (independent) methods to estimate water fluxes (e.g. current meters, acoustic Doppler current profiler (ADCP), etc.). The "internal" robustness of our estimation can be checked studying (1) the analytical error of the estimation, that is, the sensitivity of derived fluxes to perturbations of the measured variables within the limits of their respective analytical error and (2) the individual and total residuals of the estimation.

4.1. Analytical Error of the Estimation

In the case of Knudsen's hydrographic theorem (volume and salt conservation) applications, a simple analytical expression can be derived to test the effect of the error of measured variables on the estimation of horizontal residual fluxes (ε_{QS}):

$$\varepsilon_{QS} = \frac{\varepsilon_R \cdot S_B + \varepsilon_{\Delta S} + (Q_S)_S \cdot 2\varepsilon_S}{S_B - S_S}, \quad (42)$$

where ε_S is the error of the estimation of S_S or S_B. Here, ε_R and $\varepsilon_{\Delta S}$ are the errors of the estimation of Q_R+P–E and $\Delta S/\Delta t$ ($=2\varepsilon_S/\Delta t$), respectively.

For the case of volume and heat conservation, ε_{QT} is

$$\varepsilon_{QT} = \frac{\varepsilon_R \cdot |T_B - T_R| + \varepsilon_{\Delta T} + \varepsilon_H + (|(Q_S)_T| + R) \cdot 2\varepsilon_T}{|T_B - T_S|}, \quad (43)$$

where ε_T is the analytical error of the estimation T_S, T_B, or T_R. Here, ε_H and $\varepsilon_{\Delta T}$ are the analytical errors of the estimation of H and $\Delta T/\Delta t$ ($=2\varepsilon_T/\Delta t$). Similar equations can be written for volume and CO_{COR} (ε_{CO}); volume and NO_{COR} (ε_{NO}); volume and PO_{COR} (ε_{PO}); volume and NCO (ε_{NCO}); and volume and PCO (ε_{PCO}) conservation.

It is worth noting that the estimated error in equations (42) and (43) is proportional to the calculated fluxes, $(Q_S)_S$, and $(Q_S)_T$, and to the inverse of the vertical gradients, $|S_B - S_S|$ and $|T_B - T_S|$. Therefore equations (42) and (43) allow us to set the limits of the inverse method to produce reliable flux calculations, and such a limit is fixed by the number of times that the salinity gradient exceeds the accuracy of the determination, that is, it is fixed by the weighting factors, $|S_B - S_S|/\varepsilon_S$ and $|T_B - T_S|/\varepsilon_T$, of w_S and w_T.

For the case of salt–heat weighted applications, the error of the estimation ε_{QST} can be obtained analytically with the expression

$$\varepsilon_{QST} = \varepsilon_{QS} \cdot f + \varepsilon_{QT} \cdot (1 - f), \quad (44)$$

assuming that $\varepsilon_f \approx 0$. The same is applicable to calculations with any pair of conservative variables. For the case of the general salt–heat–CO–NO–PO weighted solution, the error of the estimation ε_Q is

$$\varepsilon_Q = \sum_{i=1}^{5} \varepsilon_{Q_i} \times f_i. \quad (45)$$

An equivalent expression can be written for the mass–heat–NCO–PCO optimum solution.

4.2. Representativeness Error of the Estimation

Errors calculated with equations (42)–(45) represent the expected uncertainty of the inverse method estimation in the hypothetical case that only the analytical errors of the measured variables affected the estimation. However, it is expected that the errors associated with the sampling strategy, that is, the criteria for choosing a certain number of sampling stations and depths which should be representative for the whole study system, are much larger than the analytical errors. Therefore a representativeness error, the oceanographic error ($O\varepsilon$), should be estimated and then, replacing the analytical errors (ε) by the oceanographic errors ($O\varepsilon$) in equations (42)–(44) produces:

$$O\varepsilon_Q = \sum_{i=1}^{5} O\varepsilon_{Q_i} \times f_i. \quad (46)$$

However, the proper error of the estimation (δ) is probably much lower because of the averaging effect of all terms and properties involved in the calculation of the individual errors [*Matsukawa and Suzuki*, 1985]. The proper error can be approached following the procedure of *Maamaatuaiahutapu*

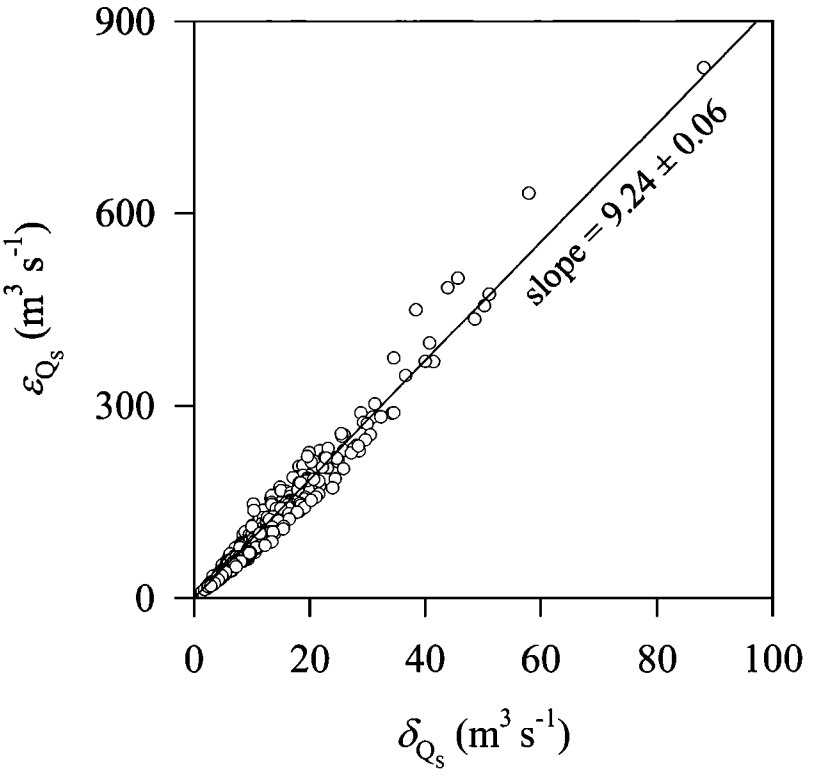

Figure 3. Oceanographic error of $(Q_S)_S$ versus proper error calculated by the perturbation method (section 4.1) for the time series of station 3 ("Ría de Vigo"; Figure 1), visited twice a week between 1987 and 1996.

et al. [1992] for the optimum multiparameter analysis of water mass composition. A number of perturbed systems of equations (11)–(17) can be obtained by random modification of the measured variables within the limits of the oceanographic errors of their estimations. One thousand perturbed systems can be produced, and 1000 different optimum solutions obtained. We obtain an average solution ($PQ = Q$) from the perturbed data and a proper error equal to the standard deviation ($\delta_{Q_\cdot} = \sigma_Q$) of the 1000 solutions.

Figure 3 shows an exercise of comparison of $O\varepsilon_{Q_S}$ obtained with equation (42) and δ_{Q_S} by perturbation of equations (11) and (13) using the 1987–1996 time series of S_S, S_B, and Q_R values for the "Ría de Vigo" (Figure 2). It should be noted that in this case S_S and S_B are not average values over the surface and bottom layer but just single values in the surface (5 m) and bottom (40 m). $\Delta S/\Delta t$ is calculated as the $(S_S + S_B)/2$ difference between two consecutive sampling dates (3–4 days), that is, it is the salinity change in the boundary rather than in the box. Finally P–E has been set to zero and $O\varepsilon_S = 0.02$, that is, 20% of ξ_S or 5 times ε_S. Despite all these simplifications, the message from Figure 3 is clear: The proper error (δ_{Q_S}) is very well correlated with the maximum expected error ($O\varepsilon_{Q_S}$) and represents about 1/4 of its value.

4.3. Individual and Total Residuals

The goodness (G) of the calculated optimum Q_S, Q_B, and NEP to fit the time changes observed in the distributions of the thermohaline and chemical (conservative or nonconservative) variables used to run the inversion can be determined by means of the expression

$$G = \sqrt{\frac{\sum_{i=1}^{I} w_i^2 \times r_i^2}{\sum_{i}^{I} \frac{(i_B - i_S)^2}{O\varepsilon_i^2}}} \quad (\mathrm{m^3\ s^{-1}}) \tag{47}$$

where i= S, T, NCO, and PCO, (I= 4) or i= S, T, CO_{COR}, NO_{COR}, and PO_{COR} (I= 5), or i= S, T, O_{2COR}, C_{TCOR}, N_{TCOR}, P_{TCOR}, and C_{TCOR} (I= 6). The residual of the volume conservation equation (r_Q) has been set to zero in all our calculations. The representation of the individual residuals (r_i) allows studying the goodness of the optimum fluxes to fit the distribution of each variable.

5. Study Case of the "Ría de Vigo" (NW Spain). Description of a Complete Upwelling-Downwelling Event in September 1990

Optimum residual fluxes and NEP rates were estimated by running OERFIM with a set of empirical data collected during a series of five consecutive surveys of the coastal upwelling system of the "Ría de Vigo" (NW Spain) in September 1990. All the required variables were measured during the surveys. In addition, surface currents were measured with a current meter, allowing validation of the calculated optimum fluxes with empirical data. OERFIM retained the solution that best describes (in a weighted least squares sense) the observed short-time scale (2–4 days) changes in the distributions of selected thermohaline and chemical tracers during a complete coastal upwelling–downwelling cycle in the NW Iberian upwelling system.

5.1. Study Area

The "Ría de Vigo" is a large (2.76 km^3) V–shaped coastal inlet freely connected with the adjacent shelf of NW Spain (Figure 1a), the northern boundary of the NW Africa/Iberian Upwelling System. Coastal winds at our latitudes (42°–43°N) are upwelling–favorable from April–May to September–October [*Wooster et al.*, 1976; *Bakun and Nelson*, 1991] and tend to occur as a succession of stress/relaxation events with a marked periodicity of 10–20 days [*Álvarez–Salgado et al.*, 1993]. The "Ría de Vigo" behaves as an inshore extension of the continental shelf during the upwelling season, with the advantage that circulation can be successfully resolved with a 2-D approach [*Prego and Fraga*, 1992; *Álvarez–Salgado et al.*, 2001].

For the purposes of this work, the study box extends from the upper reaches of the embayment (San Simon Bay, the estuary of the river Oitaben–Verdugo) to the middle ría (station 3), where the surface current meter was deployed (Figure 1a). This box is 0.53 km^3 large and presents a unique open boundary at station 3 (Figure 1b). The open boundary is divided into a surface and a bottom layer by the pycnocline. The thermohaline and chemical properties of the surface and bottom layer are calculated considering the full–depth vertical profiles collected at station 3, assuming that the embayment is transversally uniform (2-D approach). The thermohaline and chemical characteristics of the box are obtained considering measurements at stations 1, 2, and 3, as well as the geometry of the ría.

5.2. Data Set

The data used to run OERFIM came from three sources (Figure 1a): (1) the meteorological station at the airport of Vigo, (2) the buoy deployed at station 3 from September 11 to 27, 1990, and (3) the five hydrographic surveys to visit stations 1, 2, and 3 on September 14, 18, 20, 24, and 27, 1990, aboard R/V Explorador. Stations 4 and 5 were also occupied, but they will not be used in this paper.

The meteorological station at the airport provided data on rainfall (P, $m^3\ s^{-1}$) and cloudiness (N, oktas). Cloudiness is necessary to calculate the heat exchange flux across the sea surface following *Álvarez–Salgado et al.* [2001]. Continental runoff (Q_R) was computed from precipitation following *Ríos et al.* [1992].

The buoy at station 3 provided local winds (W_X and W_Y) with an Aanderaa 2740 sensor, seawater temperature at 11 depths from a thermistor chain, and surface current velocities from a RCM7 current meter. The current meter was deployed at 3.7 m, and the thermistor sensors were deployed at 2, 3.6, 4.5, 8.1, 9.5, 13.5, 14.5, 18, 19.5, 23.3 and 24.5 m. Therefore the last one was about 18 m above the bottom.

At the hydrographic stations, full–depth continuous conductivity and temperature profiles were recorded with a calibrated CTD SBE–25. Salinity was calculated from the CTD–conductivity record with the equation of *UNESCO* [1985]. The accuracy of CTD salinity and temperature was ±0.005 psu and ±0.005°C respectively. Dissolved oxygen, N nutrients, phosphate, pH and alkalinity were measured at five to seven selected depths throughout the water column at each station. Dissolved oxygen was analyzed by Winkler potentiometric end point titration, with an estimated analytical error (ε_{O_2}) of ±1 μmol kg^{-1}. Potentiometric pH was measured on the NBS scale with the classical 7.414 phosphate buffer (ε_{pH} = ±0.005) following the *Pérez and Fraga* [1987a] technique. Total alkalinity was determined by titration to pH 4.4 with 0.13 N hydrochloric acid (ε_{TA} = ±2 μmol kg^{-1}), according to the potentiometric endpoint method of *Pérez and Fraga* [1987b]. Total inorganic carbon (C_T) was calculated from pH and TA using the carbon system equation and the acid constants of *Mehrbach et al.* [1973]. The estimated ε_{CT} was ±4 μmol kg^{-1}. Nutrients were determined by segmented flow analysis following *Hansen and Grasshoff* [1983] with some small improvements [*Mouriño and Fraga*, 1985; *Álvarez–Salgado et al.*, 1992]. The corresponding analytical errors were ε_{NO2}= ±0.02 μmol kg^{-1}, ε_{NO3}= ±0.1 μmol kg^{-1}, ε_{NH4}= ±0.05 μmol kg^{-1}, ε_{SiO4}= ±0.05 μmol kg^{-1} and ε_{PO4} = ±0.01 μmol kg^{-1}. Air temperature (T_A, °C) and relative humidity (h, %) were taken from the ship to calculate the evaporation flux $E = f(h, W, T_A, T_S, S_S)$ ($m^3\ s^{-1}$) with a parametric equation [*Álvarez–Salgado et al.*, 2001].

Table 1 summarizes the meteorological, thermohaline, and chemical data for the three boundaries (continent, atmosphere, and wall) and the volume of the study box necessary to run the conservative and nonconservative versions of OERFIM. Four periods are considered, September 14–18, 18–20, 20–24, and 24–27, 1990.

5.3. Hydrographic Scenario in the Ría de Vigo During September 1990

As for any coastal upwelling system, the offshore Ekman transport ($-Q_X$) is the main forcing agent of the residual circulation in the "Ría de Vigo" [*Álvarez–Salgado et al.*, 2000; *Pardo et al.*, 2001]. Ekman transport values were obtained from wind data at the Cape Finisterre meteorological station (Figure 1a) and the equation of *Wooster et al.* [1976],

$$-Q_X = -\frac{\rho_{air} \times C_D \times \sqrt{W_X^2 + W_Y^2} \times W_Y}{\rho_{sw} \times f}, \qquad (48)$$

where ρ_{air} is the density of air, 1.22 kg m^3 at 15°C; C_D is an empirical drag coefficient (dimensionless), 1.3 10^{-3} according to *Hidy* [1972]; f is the Coriolis parameter, 9.946 10^{-5} s^{-1} at 43°N latitude; ρ_{sw} is the density of seawater, ~1025 kg m^3, and W_X and W_Y in m s^{-1} are the south–north and west–east components of the coastal winds at Cape Finisterre. Local winds provided by the buoy are not representative for the wind patterns off the "Ría de Vigo", because the embayment is well protected by the surrounding mountains, more than 400 m high.

Figure 4 presents an excellent picture of the succeeding hydrographic scenarios in the 'Ría de Vigo' during the second fortnight of September 1990, at the time of the transition from upwelling–favorable northerly winds to downwelling–favourable southerly winds. Figure 4a shows the time course of the offshore Ekman transport (3 days running mean). An evolution is clearly observed from a situation of wind calm on September 14 to an upwelling peak on September 17, a subsequent upwelling relaxation to September 24 and, finally, a strong downwelling event that culminates on September 27 1990. Figure 4b shows the response of the water column to coastal winds. The 14°–15°C isotherms paralleled the time evolution of $-Q_X$ from September 14 to 24. The subsequent downwelling event allows the downward penetration of surface water warmer than 17°C up to 20 m depth. Finally, Figure 4c completes the picture, showing the progressive

Table 1. Data Set to Run OERFIM Box Model in the "Ría de Vigo" During September 1990.

Continental Runoff Tracer Values

Interval Days	S_R, kg m^{-3}	T_R, °C	N_{TR}, mmol m^{-3}	P_{TR}, mmol m^{-3}	C_{TCORR}, mmol m^{-3}	O_{2CORR}, mmol m^{-3}	NCO_R, mmol m^{-3}	PCO_R, mmol m^{-3}
14–18	0.00	21.85	46.0	1.0	44.8	244.5	415	333
18–20	0.00	21.49	46.0	1.0	44.8	246.5	421	339
20–24	0.00	19.62	46.0	1.0	44.8	256.5	426	344
24–27	0.00	19.53	46.0	1.0	44.8	256.5	424	342

Atmospheric Tracer Values

Interval Days	S_A, kg m^{-3}	T_A, °C	N_{TA}, mmol m^{-3}	P_{TA}, mmol m^{-3}	C_{TCORA}, mmol m^{-3}	O_{2CORA}, mmol m^{-3}	NCO_A, mmol m^{-3}	PCO_A, mmol m^{-3}
14–18	0.00	21.85	0	0	0	0	0	0
18–20	0.00	21.49	0	0	0	0	0	0
20–24	0.00	19.62	0	0	0	0	0	0
24–27	0.00	19.53	0	0	0	0	0	0

Tracer Values at the Surface Wall (Station 3)

Interval Days	S_S, kg m^{-3}	T_S, °C	N_{TS}, mmol m^{-3}	P_{TS}, mmol m^{-3}	C_{TCORS}, mmol m^{-3}	O_{2CORS}, mmol m^{-3}	NCO_S, mmol m^{-3}	PCO_S, mmol m^{-3}
14–18	35.39	17.22	3.9	0.41	922	252	1184	1191
18–20	35.52	16.76	5.8	0.58	936	223	1175	1184
20–24	35.57	16.65	3.8	0.35	914	245	1169	1174
24–27	35.50	17.44	0.9	0.09	879	270	1147	1148

Tracer Values at the Bottom Wall (Station 3)

Interval Days	S_B, kg m^{-3}	T_B, °C	N_{TB}, mmol m^{-3}	P_{TB}, mmol m^{-3}	C_{TCORB}, mmol m^{-3}	O_{2CORB}, mmol m^{-3}	NCO_B, mmol m^{-3}	PCO_B, mmol m^{-3}
14–18	35.73	14.32	9.2	0.72	975	195	1194	1201
18–20	35.74	14.18	9.2	0.68	971	191	1187	1191
20–24	35.69	15.00	8.9	0.74	966	184	1175	1182
24–27	35.61	16.19	7.3	0.73	954	189	1156	1167

Tracer Box Time Derivatives

Interval Days	$V\frac{\Delta S}{\Delta t}$, kg s^{-1}	$V\frac{\Delta T}{\Delta t}$, °C m^3 s^{-1}	$V\frac{\Delta N_T}{\Delta t}$, Mmol s^{-1}	$V\frac{\Delta P_T}{\Delta t}$, mmol s^{-1}	$V\frac{\Delta C_{TCOR}}{\Delta t}$, mmol s^{-1}	$V\frac{\Delta O_{2COR}}{\Delta t}$, mmol s^{-1}	$V\frac{\Delta NCO}{\Delta t}$, mmol s^{-1}	$V\frac{\Delta PCO}{\Delta t}$, mmol ·s^{-1}
14–18	194	−903	4446	387	35895	−68788	−20770	−16236
18–20	147	−1455	3184	138	24945	−29319	5167	2452
20–24	−165	1888	−7618	−593	−89215	80548	−29898	−34621
24–27	−85	1287	−1774	−156	−17394	9591	−23424	−26370

Atmosphere–Sea Exchange Fluxes and Continental Runoff

Interval Days	P, m^3 s^{-1}	E, m^3 s^{-1}	Q_R, m^3 s^{-1}	H, °C m^3 s^{-1}	F_{CO_2}, mmol s^{-1}	F_{O_2}, mmol s^{-1}	F, mmol s^{-1}
14–18	0.01	0.050	3.8	1009	−3.9	−4197	−1202
18–20	0.53	0.000	3.7	1061	−13.7	4413	1251
20–24	1.31	0.129	7.1	595	−19.3	−3749	−1085
24–27	0.00	0.175	10.6	650	−5.0	−13070	−3738

vector diagram for the near–surface current meter. The data were filtered with a 3 day running mean. Therefore tidal effects were completely erased prior to calculating the progressive vector. The direction of the observed currents is quasi–parallel to the main axis of the ría, supporting the 2-D approach. In agreement with the time evolutions of $-Q_X$ and temperature, from September 12 to 15 warm shelf surface water entered the ría up to station 3. From September 15 to 21 the warm surface waters flowed out of the ría and the temperature of the embayment decreased to its minimum

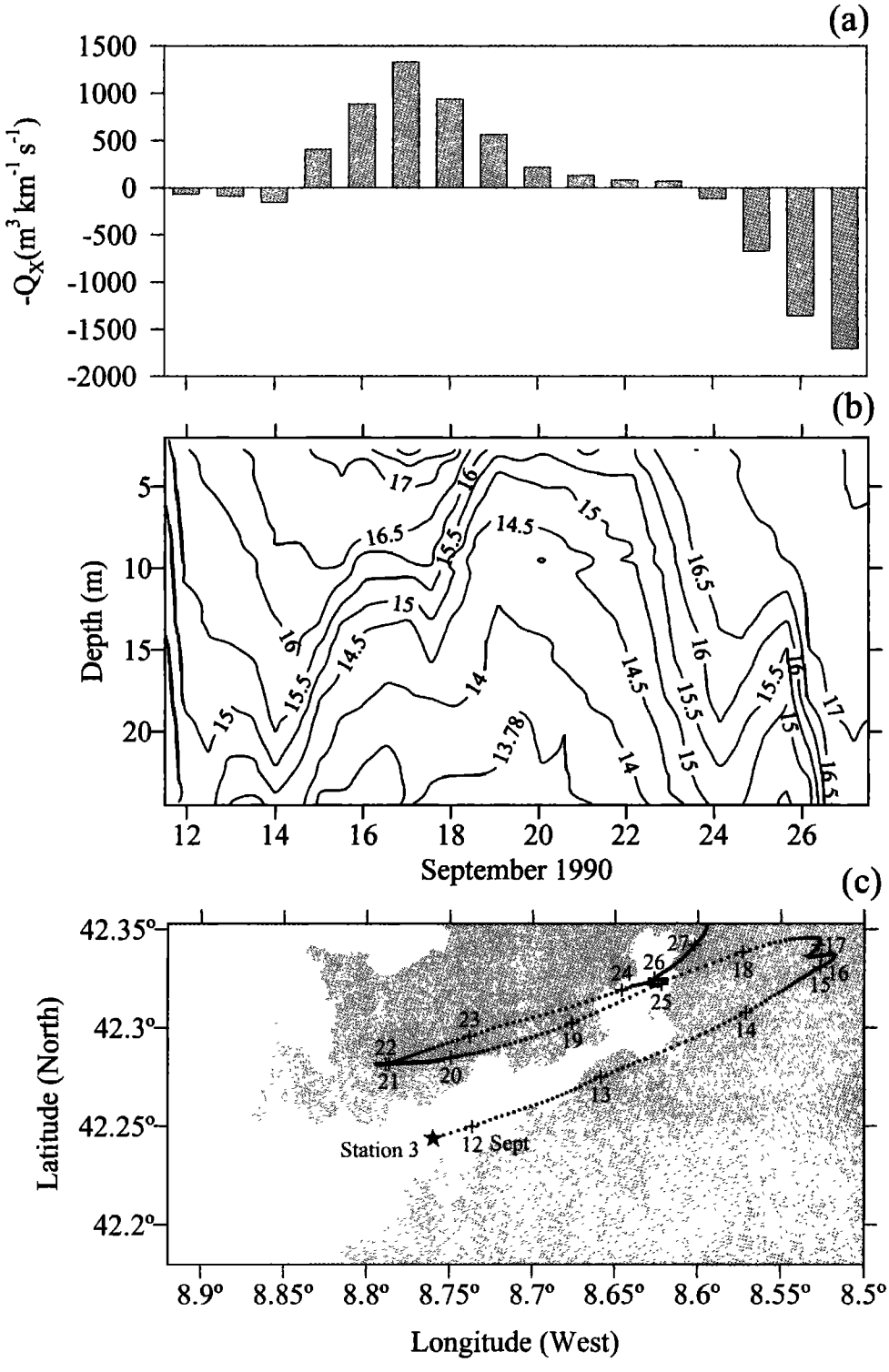

Figure 4. (a) Offshore Ekman transport ($-Q_X$) calculated with winds at the Cape Finisterre meteorological station and filtered with a 3 day running mean ($m^3\ s^{-1}\ km^{-1}$). (b) Time evolution of the temperature profile at station 3 from thermistor chain record (°C). (c) Progressive vector diagram for the near-surface (3.7 m deep) current meter at station 3 during the study period in September 1990. The velocity data were filtered with a 3 day running mean. The numbers indicate the day of September (00:00 hours).

because of wind–driven upwelling. Finally, from September 21 to 27 the surface circulation reversed again in response to the upwelling relaxation and subsequent strong downwelling.

5.4 Results From the Conservative Version of OERFIM (*S*, *T*, NCO, and PCO)

Optimum Q_S and Q_B values were calculated using the required data (Table 1) to solve the system of equations (38)–(40), the analytical errors being $\varepsilon_T = 0.005$°C, $\varepsilon_S = 0.005$ psu, and $\varepsilon_{NCO} = \varepsilon_{PCO} = 7.4$ μmol kg^{-1}. The oceanographic errors of the estimation, $O\varepsilon_{Q_S}$ and $O\varepsilon_{Q_B}$, were obtained with equation (46) with $O\varepsilon_i = 0.2 \times \xi_i$ (i= *S*, *T*, NCO and PCO). Twenty percent of ξ_i seems a reasonable oceanographic error, since the spatial and temporal hydrographic variability of the "Ría de Vigo" affects essentially the vertical rather than the horizontal profiles of the thermohaline and chemical variables. The representativeness error for the other variables, river and atmosphere fluxes, was set to 10% of the corresponding measured/estimated value of the variable The results are presented in Table 2. In addition, the average (PQ_S, PQ_B) and standard deviation (δ_{PQ_S}, δ_{PQ_B}) of the set of 1000 solutions obtained with the perturbation method (section 4.2) are also summarized in Table 2. It is clear that the maximum expected errors are about 4 times the proper error, as in Figure 3.

Figure 5a shows the time evolution of f_i, indicating that Q_S and Q_B in the study case depended mainly on the temperature budget. Values of f_S, f_{NCO} and f_{PCO} are so low that the solution retained by the conservative version of OERFIM does not differ substantially from the solution arising from equations (26) and (27). The reason behind the observed behavior is the homogeneous vertical distributions of NCO, PCO, and salinity compared with temperature, as suggested by Table 1. Since continental runoff was quite limited (<11 m^3 s^{-1}), the ría was primarily occupied by cold and salty Eastern North Atlantic Central Water (ENACW) with constant NCO and PCO concentrations. Heat exchange across the sea surface (*H*, Table 1) contributes to warm the surface layer, enhancing the temperature gradient but producing no effect on the salinity, NCO, and PCO profiles. These tracers acquire more relevance for the calculation of optimum estuarine fluxes when continental runoff is higher, as occurs during the winter in the "Ría de Vigo" or throughout the year in most of the estuaries of large rivers.

5.5 Results From Nonconservative Version of OERFIM (S,T, O_{2COR}, C_{TCOR}, N_T and P_T)

Optimum horizontal residual fluxes (Q_S, Q_B) were obtained again at station 3 by solving the overdetermined system of equations (11)–(17) as indicated in section 3.4 (equation (41)). In addition, optimum net ecosystem production rates within the study box (NEP) were simultaneously obtained. The required data are summarized in Table 1, and the corresponding results are presented in Table 3. Matrices $\boldsymbol{A}$ and $\boldsymbol{B}$ were randomly perturbed 1000 times within the error limits of the measured/estimated variables, and again $O\varepsilon_i = 0.2 \times \xi_i$ with i= *S*, *T*, O_{2COR}, C_{TCOR}, N_T, and P_T, and 10% of the measured/estimated value for the rest of variables. The w_i terms of the diagonal matrix $\boldsymbol{W}$ were calculated with $\varepsilon_T = 0.005$°C, $\varepsilon_S = 0.005$ psu, $\varepsilon_{N_T} = 0.1$ μmol kg^{-1}, $\varepsilon_{P_T} = 0.01$ μmol kg^{-1}, $\varepsilon_{C_{TCOR}} = 4.5$ μmol kg^{-1} and $\varepsilon_{O_{2COR}} = 1.1$ μmol kg^{-1}. The corresponding average (PQ_S, PQ_B, *P*NEP) and standard deviation (δ_{PQ_S}, δ_{PQ_B}, δ_{PNEP}) of the 1000 solutions are also presented in Table 3.

Although f_i values for the nonconservative version of OERFIM have not been derived, pseudo values of f_i can be calculated for O_{2COR}, C_{TCOR}, N_T, and P_T with equation (40). Despite the pronounced vertical gradients of the nonconservative variables (Table 1), the retained solution is again controlled by the extreme temperature gradients (Figure 5b). However, for the September 24–27 period the contribution of O_{2COR}, N_T, and P_T became more important because of the relative thermal homogenization caused by strong downwelling events (Figure 4b) and the enhanced gradients of the non conservative tracers (Table 1). In any case, Q_S and Q_B are not substantially different from the values obtained with the conservative version of OERFIM. Obviously, the major differences are obtained for the last study period.

The obtained NEP rates are coherent with the expected time evolution during an upwelling–downwelling sequence. NEP is negative, that is, respiration exceeds production, during the spin-up phase of upwelling. It become practically nil during the upwelling climax and increased dramatically, that is, production exceeded respiration, during the subsequent upwelling relaxation. Finally, respiration is again dominant under downwelling conditions. The lag time between NEP and upwelling is related to the low initial phytoplankton biomass in recently upwelled water [*Brown and Field*, 1986] and the large flushing rates (Figure 4c; Table 3), which do not allow complete transition from slow to fast phytoplankton growth in response to the new high nutrient and light conditions [*Zimmerman et al.*, 1987]. On the other hand, downwelling periods usually are dominated by respiration processes [*Pérez et al.*, 2000].

5.6. Comparison of Optimum Fluxes and Measured Surface Current.

The reasonable errors of the residual fluxes and net ecosystem production rates (Table 3) prove the robustness of

Table 2. Results From OERFIM Box Model With Conservative Equations (NCO and PCO) in the "Ría de Vigo" During September 1990.

Interval Days	Q_S, m^3 s^{-1}	$O\varepsilon_{Q_S}$, m^3 s^{-1}	Q_B, m^3 s^{-1}	$O\varepsilon_{Q_B}$, m^3 s^{-1}	G, m^3 s^{-1}	PQ_S, m^3 s^{-1}	δ_{PQ_S}, m^3 s^{-1}	PQ_B, m^3 s^{-1}	δ_{PQ_B}, m^3 s^{-1}
14–18	675	±161	671	±161	100	679	±47	675	±47
18–20	991	±253	986	±254	62	992	±74	987	±74
20–24	–755	±340	–763	±341	149	–759	±101	–767	±101
24–27	–459	±324	–470	±325	287	–465	±85	–475	±85

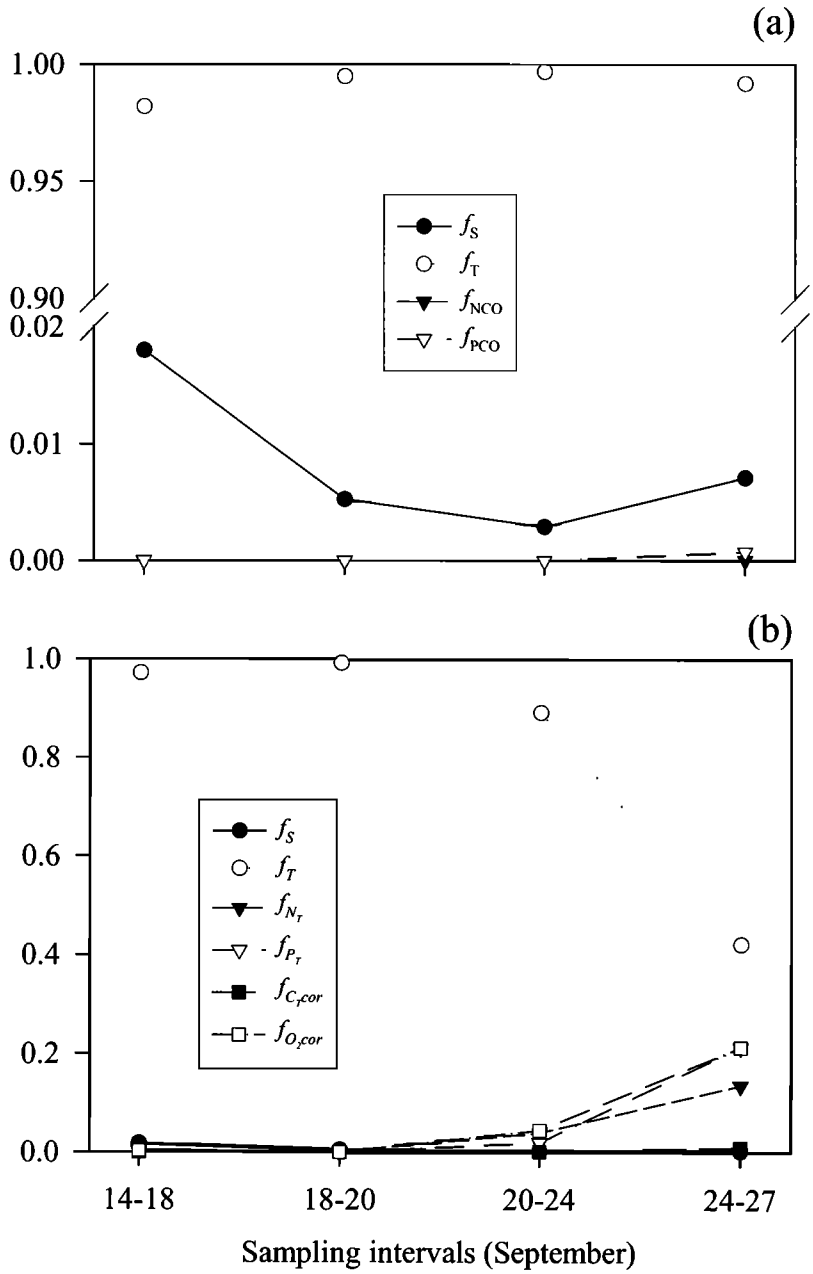

Figure 5. Plots of f_i for the (a) conservative and (b) nonconservative versions of OERFIM applied to the data from the Ría de Vigo in September 1990.

the solutions retained by OERFIM. In addition, we have the opportunity to test the accuracy of the estimation of Q_S by comparing the retained solution (PQ_S), converted to velocity (PV_S) considering the cross section of the surface layer of the wall, with the measured surface currents at station 3 (Figure 6). The agreement is good, though for the September 18–20 period OERFIM underestimates the outgoing velocity under intense upwelling conditions when the 2-D approach could be weaker. In any case, it should be considered that results from direct current measurements indicate water displacements at a

Table 3. Results From OERFIM Box Model With Nonconservative Equations (N_T, P_T, C_{Tcor}, O_{2cor}) in the "Ría de Vigo" During September 1990.

Interval	Q_S,	Q_B,	NEP,	G,	PQ_S,	δ_{PQ_S},	PQ_B,	δ_{PQ_B},	PNEP,	δ_{PNEP},
days	$m^3 s^{-1}$	$m^3 s^{-1}$	$gC m^2 d^{-1}$	$m^3 s^{-1}$	$m^3 s^{-1}$	$m^3 s^{-1}$	$m^3 s^{-1}$	$m^3 s^{-1}$	$gC m^2 d^{-1}$	$gC m^2 d^{-1}$
14–18	675	671	−0.38	118	677	±45	673	±45	−0.37	±0.08
18–20	991	986	0.03	65	994	±74	990	±74	0.04	±0.08
20–24	−756	−764	0.94	149	−759	±102	−767	±102	0.93	±0.16
24–27	−441	−452	−0.29	273	−434	±75	−444	±75	−0.28	±0.14

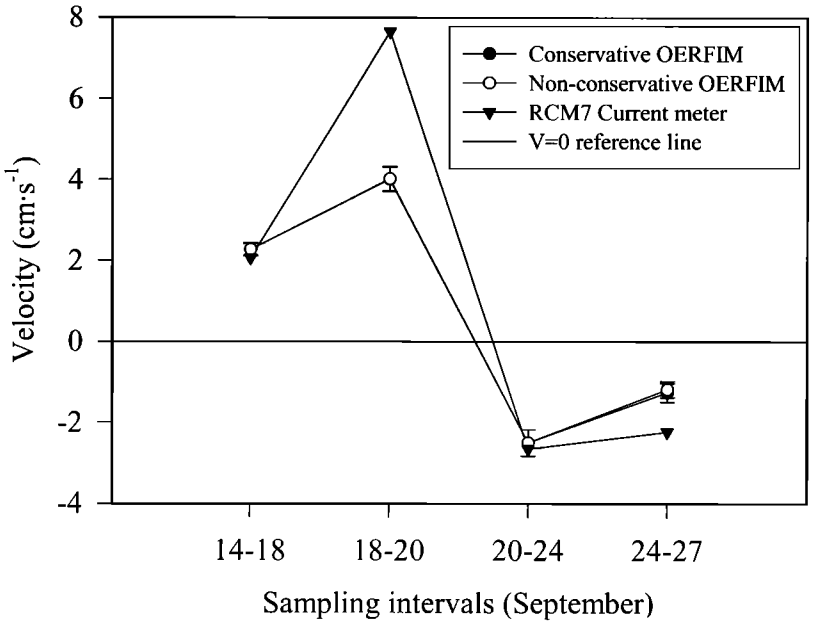

Figure 6. Comparison between surface OERFIM velocities solutions and surface RCM7 current meter average velocities perpendicular to the box wall at station 3.

given position and depth, whereas OERFIM fluxes are representative for a cross sections of 3.05 10^4 m^2.

6. Conclusions

OERFIM is an optimum multiparameter update of the classical box models, which is revealed to be a useful research tool for the simultaneous estimation of residual fluxes and net ecosystem production (NEP) rates in partially mixed estuaries, coastal inlets, and enclosed seas. Compared with classical box models, OERFIM combines all the thermohaline and chemical information usually available from the abundant hydrographic studies of these relevant marine systems to obtain optimum, appropriately weighted, solutions, not only of residual fluxes but of NEP rates too. Knowledge of the analytical solutions of OERFIM allows us to define a specific normalizing-weighting factor (w_i) instead of using sophisticated procedures such as single-value decomposition, tapered least squares, or other numerical methods [*Wunsch*, 1996]. In any case, the normalizing factor (ξ_i), mimics the classical weighting factor used in the literature about inverse methods: the variance of the residuals. Moreover, OERFIM pays particular attention to the reliability of the results, incorporating a rigorous assessment of the analytical, oceanographic, and perturbed errors of the system of balance equations and their intricate relationships. It is concluded that the perturbed error is the more appropriate parameter to assess the consistency of the solutions produced by OERFIM because of the averaging effect of all terms and properties involved in the calculation of the individual error of each thermohaline and chemical variable. This also is also a substantial improvement compared with the classical box models, which usually consider only one state variable (salinity or temperature).

Finally, the first step of OERFIM, the 0-D solution, is applied to a set of field data collected in the Ría de Vigo, a coastal inlet off NW Spain affected by intermittent upwelling/downwelling events. The optimum solution provided by OERFIM is reasonably accurate and reliable regarding either the water fluxes or the NEP rates. Estimated residual fluxes compare fairly well with the concurrent current meter record and the uncertainty of the solution (the perturbed error) stays within an acceptable interval. It is also shown that OERFIM provides useful information on the structure of the solution from the f_i factors.

Acknowledgments. The authors wish to thank the crew and scientific parties that joined the surveys of the "Ría de Vigo" during September 1990 aboard R/V "Explorador". Special thanks to G. Rosón and T. Rellán for inorganic carbon and dissolved oxygen analyses, B.M. Miguez for the calculation of average tracer concentrations in boxes and boundaries, and the Dunstaffnage Marine Laboratory for instrument and mooring development and processing of the buoy data. We are also very grateful to Fabienne Gaillard and Herlé Mercier at LPO (IFREMER), where M. Gilcoto learned a lot about inverse methods and matured some of the ideas here exposed. Support for this work came from the EU project MAST-CT90-0017 (The Control of Phytoplankton Dominance). Comments by two anonymous reviewers are very much appreciated.

References

Álvarez-Salgado, X.A., F.F. Pérez, and F. Fraga, Determination of nutrient salts by automatic methods both in seawater and brackish water: The phosphate blank, *Mar. Chem., 39*, 311–319, 1992.

Álvarez-Salgado, X.A., G. Rosón, F.F. Pérez, and Y. Pazos, Hydrographic variability off the Rías Baixas (NW Spain) during the upwelling season, *J. Geophys. Res., 98*, 14,447–14,455, 1993.

Álvarez-Salgado, X.A., J. Gago, B.M. Míguez, M. Gilcoto, and F.F. Pérez, Surface waters of the NW Iberian margin: Upwelling on the shelf versus outwelling of upwelled waters from the Rías Baixas, *Estuarine Coastal Shelf Sci., 51*, 821–837, 2001.

Anderson, L.A., On the hydrogen and oxygen content of marine phytoplankton, *Deep Sea Res., Part I, 42*, 1675–1680, 1995.

Anderson, L.A., and J.L. Sarmiento, Redfield ratios of mineralization determined by nutrient data analysis, *Global Biogeochem. Cycles, 8*, 65–80, 1994.

Bakun, A., and C.S. Nelson, The seasonal cycle of wind-stress curl in subtropical eastern boundary current regions, *J Phys. Oceanogr., 21*, 1815–1834, 1991.

Broecker, W.S., "NO" a conservative water-mass tracer, *Earth Planet. Sci. Lett., 23*, 100–107, 1974.

Broecker, W.S., and T.-H. Peng, *Tracers in the Sea*, 690 pp., Lamont-Doherty Earth Observatory, Palisades, N.Y., 1982.

Brown, P.C., and J.G. Field, Factors limiting phytoplankton production in a nearshore upwelling area, *J. Plankton Res.*, *8*, 55–68, 1986.

Fiadeiro, M. E., and G. Veronis, On the determination of absolute velocities in the ocean, *J. Mar. Res*, *40*(Suppl.), 159–182, 1982.

Fraga, F., F.F. Pérez, F.G. Figueiras, and A F. Ríos, Stoichiometric variations of N, P, C, and O_2 during a *Gymnodinium catenatum* red tide and their interpretation, *Mar. Ecol. Prog. Ser*, *87*, 123–134, 1992.

Fraga, F., A.F. Ríos, F.F. Pérez, M. Estrada, and C. Marrasé, Effect of upwelling pulses on excess carbohydrate synthesis as deduced from nutrient, carbon dioxide and oxygen profiles, *Mar. Ecol. Prog. Ser.*, *189*, 65–75, 1999.

Grose, T.J., G R. Bigg, and J.A Johnson, The Bernoulli inverse method. Theory and practice, *Deep Sea Res., Part I*, *41*, 767–785, 1994.

Hansen, H.P., and K. Grasshoff, Automated chemical analysis, in *Methods of Seawater Analysis*, 2nd ed., edited by K. Grasshoff, M. Ehrhardt, and K. Kermling, pp. 347–395, Verlag Chem, Weinheim, Germany, 1983.

Hidy, G.M., A view of recent air–sea interaction research, *Bull. Am. Meteorol. Soc.*, *53*, 1083–1102, 1972.

Karstensen, J., and M. Tomczak, Ventilation processes and waters mass ages in the thermocline of the southeast Indian Ocean, *Geophys. Res Lett.*, *24*, 2777–2780, 1997.

Kester, D R., Dissolved gases other than CO_2, in *Chemical Oceanography*, vol. 1, 2nd ed., edited by J.P. Riley and G. Skirrow, pp. 497–556, Academic, San Diego, Calif.,1975.

Maamaatuaiahutapu, K., V.C. Garçon, C. Provost, M. Boulahdid, and A.P. Osiroff, Brazil–Malvinas confluence: Water mass composition, *J. Geophys. Res*, *97*, 9493–9505, 1992.

Mackas, D.L., K.L. Denman, and A.F. Bennett, Least squares multiple tracer analysis of water mass composition, *J. Geophys. Res*, *92*, 2907–2918, 1987.

Matsukawa, Y., and T. Suzuki, Box model analysis of hydrography and behavior of nitrogen and phosphorus in an eutrophic estuary, *J. Oceanogr. Soc. Jpn*, *41*, 407–426, 1985

Mazé, J.P., M. Arhan, and H. Mercier, Volume budget of the eastern boundary layer off the Iberian Peninsula, *Deep Sea Res., Part I*, *44*, 1543–1574, 1997.

Mehrbach, C., C.H. Culberson, J.E. Hawley, and R.M. Pytkowitcz, Measurements of the apparent dissociation constants of carbonic acid in seawater at atmospheric pressure, *Limnol. Oceanogr*, *18*, 897–906, 1973.

Mercier, H., Determining the general circulation of the ocean: A nonlinear inverse problem, *J. Geophys. Res.*, *91*, 5103–5109, 1986.

Minas, H.J., M. Minas, and T.T. Packard, Productivity in upwelling areas deduced from hydrographic and chemical fields, *Limnol. Oceanogr.*, *31*, 1182–1206, 1986.

Mouriño, C., and F. Fraga, Determinación de nitratos en agua de mar, *Invest. Pesq*, *49*, 81–96, 1985.

Neumann, G., and W.J. Pierson Jr., *Principles of Physical Oceanography*, 545 pp., Prentice–Hall, Englewood Cliffs, N. J., 1967.

Officer, C.B., Box models revisited, in *Estuarine and Wetlands Processes With Emphasis on Modelling*, edited by P. Hamilton and K.B. McDonald, pp. 65–114, Plenum, New York, 1980.

Pardo, P.C., M. Gilcoto, and Fiz F. Pérez, Short–time scale coupling between termohaline and meteorological forcing in the Ría de Pontevedra, *Sci. Mar.*, *65* (Suppl. 1), 229-240, 2001.

Pérez, F.F., and F.F. Fraga, The pH measurements in seawater on NBS scale, *Mar. Chem.*, *21*, 315–327, 1987a.

Pérez, F.F., and F. Fraga, A precise and rapid analytical procedure for alkalinity determinations, *Mar. Chem.*, *21*, 169–182, 1987b.

Pérez, F.F., X.A. Álvarez–Salgado, and G. Rosón, Stoichiometry of net ecosystem metabolism in coastal inlet affected by upwelling: The Ría de Arousa (NW Spain), *Mar. Chem.*, *69*, 217–236, 2000.

Prego, R., and F. Fraga, A simple model to calculate the residual flows in a Spanish ría. Hydrographic consequences in the Ría of Vigo, *Estuar. Coast. Shelf Sci.*, *34*, 603–615, 1992.

Pritchard, D.W., Dispersión and flushing of pollutants in estuaries, *J. Hydraul Div. Am. Soc. Civ. Eng.*, *95*, 115–124, 1969.

Redfield, A.C., B.H Ketchum, and F.A. Richards, The influence of organisms on the composition of sea–water, in *The Sea*, vol. 2, *Composition of Sea Water*, edited by M.N. Hill, pp. 26–77, John Wiley, New York, 1963.

Ríos, A.F., F. Fraga, and F.F. Pérez, Estimation of coefficients for the calculation of "NO", "PO" and "CO", starting from the elemental composition of natural phytoplankton, *Sci. Mar.*, *53*, 779–784, 1989.

Ríos, A.F., M.A. Nombela, F.F. Pérez, G. Rosón, and F. Fraga, Calculation of runoff to an estuary: Ría de Vigo, *Sci. Mar*, *56*, 29–33, 1992.

Rosón, G., X.A. Álvarez–Salgado, and F.F. Pérez, A nonstationary box model to determine residual fluxes in a partially mixed estuary, based on both thermohaline properties: Application to the Ria de Arousa (NW Spain), *Estuarine Coastal Shelf Sci.*, *44*, 249–262, 1997.

Smith, S.V., and J.T. Hollibaugh, Annual cycle and interannual variability of ecosystem metabolism in a temperate climate embayment, *Ecol Monogr.*, *67*, 509–533, 1997.

Spencer, C.P., The micronutrient elements, in *Chemical Oceanography*, 2nd ed., edited by J.P. Riley and G. Skirrow, pp. 245–300, Academic, San Diego, Calif., 1975.

Taft, J.L., A.J. Elliott, and W.R. Taylor, Box model analysis of Chesapeake by ammonium and nitrate fluxes, in *Estuarine Interactions*, edited by M.J. Wiley, pp. 115–130, Academic, San Diego, Calif., 1978.

Takahashi, T., W.S. Broecker, and S. Langer, Redfield ratio based on chemical data from isopycnal surfaces, *J Geophys Res.*, *90*, 6907–6924, 1985

Tarantola, A., and B. Valette, Generalized nonlinear inverse problems solved using the least squares criterion, *Rev. Geophys.*, *20*, 219–232, 1982.

Thompson, R.O.R.Y., and R.J. Edwards, Mixing and water–mass formation in the Australian subantarctic, *J. Phys. Oceanogr.*, *11*, 1399–1406, 1981.

Tomczak, M., A multi–parameter extension of temperature/salinity diagrams technique for the analysis of nonisopycnal mixing, *Prog. Oceanogr.*, *10*, 147–171, 1981.

Tomczak, M., Some historical, theoretical and applied aspects of quantitative water mass analysis *J. Mar. Res.*, *57*, 275–303, 1999.

UNESCO, The international system of units (SI) in oceanography, *UNESCO Tech. Pap. Mar. Sci.*, *45*, Paris, 1985.

Weiss, R.F., Carbon dioxide in water and seawater: The solubility of a non-ideal gas, *Mar. Chem.*, *2*, 203–215, 1974.

Woolf, D.K., and S.A. Thorpe, Bubbles and the air–sea exchange of gases in near–saturation conditions, *J. Mar. Res.*, *49*, 435–466, 1991.

Wooster, W.S., A. Bakun, and D.R. Mclain, The seasonal upwelling cycle along the eastern boundary of the North Atlantic, *J. Mar. Res*, 34, 131–141, 1976.

Wunsch, C., Determining the general circulation of the oceans: A preliminary discussion, *Science*, *196*, 871–875, 1977.

Wunsch, C., The North Atlanctic general ciculation west of 50°W determined by inverse methods, *Rev. Geophys.*, *16*, 583–620, 1978.

Wunsch, C., Eclectic modelling of the North Atlanctic, II, Transient tracers and the ventilation of the Eastern Basin thermocline, *Philoso. Trans R. Soc. Lond. on, Ser. A*, *325*, 201–236, 1988.

Wunsch, C., *The Ocean Circulation Inverse Problem*, 442 pp., Cambridge Univ. Press, New York, 1996.

Wunsch, C., and J.-F. Minster, Methods for box models and ocean circulation tracers: Mathematical programming and nonlinear inverse theory, *J. Geophys. Res.*, *87*, 5647–5662, 1982.

Zimmerman, R.C., J.N. Kremer, and R.C. Dugdale, Acceleration of nutrient uptake by phytoplankton in a coastal upwelling ecosystem: A modeling analysis. *Limnol. Oceanogr.*, *32*, 359–367, 1987.

X. A. Álvarez-Salgado, M. Gilcoto, and F. F. Pérez, Instituto de Investigacións Mariñas, Eduardo Cabello 6, 36208, Vigo, Spain. (xasalgado@iim.csic.es, migil@iim.csic.es, fiz@iim.csic.es)

(Received October 2, 2000; revised June 18, 2001; accepted June 18, 2001.)